Optimum placement of post-1PN gravitational wave chirp templates made simple at any match level via Tanaka-Tagoshi coordinates

R. P. Croce
Wavesgroup, D.I.³E., University of Salerno, Italy

Th. Demma, V. Pierro, and I. M. Pinto
Wavesgroup, University of Sannio at Benevento, Italy

A simple recipe is given for constructing a maximally sparse regular lattice of spin-free post-1PN gravitational wave chirp templates under a given minimal-match constraint, using Tanaka-Tagoshi coordinates. Cardinal interpolation among the resulting maximally sparse templates is discussed.

I. INTRODUCTION

Gravitational wave *chirps* emitted by compact binary stars in their adiabatic inspiral phase will be primary targets for the early operation of broadband laser-interferometric detectors such as TAMA300, GEO600, the Laser Interferometric Gravitational Wave Observatory (LIGO) and VIRGO [1]. These signals have been thoroughly studied and accurately modeled [2].

The maximum-likelihood strategy [3] for detecting signals of known shape (except for a set of unknown parameters) in additive stationary colored Gaussian noise consists in correlating the data with a set $\mathcal{L} = \{g_i\}$ of possible expected waveforms (*templates*) and using the largest correlator as a detection statistic [3]. The mentioned correlators are the (noise-weighted) scalar products

$$\langle a, g \rangle = 2 \left[\int_{f_i}^{f_s} a(f) g^*(f) \frac{df}{\Pi(f)} + \text{c.c.} \right], \qquad (1.1)$$

where (f_i, f_s) is the antenna spectral window, $a(f) = h(f) + n(f)$ are the noise-corrupted (spectral) data, $h(f)$ is a (possibly null) signal, $n(f)$ is a realization of the antenna noise with (one-sided) power spectral density $\Pi(f)$, $g(f)$ is a template, and c.c. denotes complex conjugation.

The issue of optimum placement of the templates in the waveform parameter space is more or less obviously a crucial and still open one, and has been addressed by several authors [4–8].

At fixed false-alarm probability, the detection probability is an increasing function of the *overlap*

$$\mathcal{O}(h, g) = \frac{\langle h, g \rangle}{||h|| \cdot ||g||} \leq 1 \qquad (1.2)$$

between the signal h and the template g, where the norm $||u|| = \langle u, u \rangle^{1/2}$. The template set $\mathcal{L}$ should be designed in such a way that, for any admissible signal h, the overlap never drops below a prescribed value Γ, which can be immediately related to the fraction $(1 - \Gamma^3)$ of potentially observable sources which might be missed out [6].

The overlap can be readily maximized with respect to the (unknown but irrelevant) initial-phase and coalescency-time

differences between the signal and the template [9]. The resulting partially maximized overlap is called the *match*, is denoted by $M(h, g)$, and is a function of the source and template *intrinsic* parameters only (e.g., at 2.5PN order, the binary companion masses, spin-spin and spin-orbit parameters). The minimum-overlap condition rephrases obviously into the following minimal-match prescription:

$$\forall h \in \mathcal{S}, \quad \exists g \in \mathcal{L} : M(h, g) \geq \Gamma, \qquad (1.3)$$

where $\mathcal{S}$ is the set of admissible signals.

Discussion will be henceforth restricted to the 2D parameter space of spin-free chirp-waveforms, in view of the widespread present consensus that these should be adequate for the early operation of interferometric detectors [8].

In the following we shall denote as G the (2D, spin-free) parameter-space point corresponding to waveform g. We shall also denote as $\gamma_\Gamma(G)$ the match contour line, whose points represent the set of waveforms h such that $M(h, g) = \Gamma$, and as $S_\Gamma(G)$ the 2D region bounded by $\gamma_\Gamma(G)$, representing the set of waveforms h such that $M(h, g) \geq \Gamma$.

The template set $\Lambda = \{G_i\}$ should satisfy the following basic requirements. First of all, (a) the minimal-match condition (1.3) should be met, which rephrases into

$$\cup_i S_\Gamma(G_i) \supseteq \Sigma, \qquad (1.4)$$

where Σ is the image of $\mathcal{S}$, i.e. the subset of the waveform parameter-space corresponding to admissible sources. Pictorially, Eq. (1.4) means that the patches $S_\Gamma(G_i)$ should cover the whole set Σ without leaving holes. At the same time, (b) the template set Λ should be chosen *as much sparse as possible*, so as to minimize the overall number of templates, and hence the detection threshold level, for any prescribed false-alarm probability [3].

It might be further desirable (c) to deal with a set Λ forming a regular (or piecewise-regular) grid, for computational ease.

A further template-placement requirement is also worth mentioning. When covering Σ with (regularly spaced or patch-wise regularly spaced) templates, a certain amount of template spillover beyond $\partial\Sigma$ is unavoidable. The post-1PN spin-free waveform parameter-space subset Σ corresponding

to admissible sources, for which $m_{min} \leq m_1 \leq m_2 \leq m_{max}$, is a three-vertex curved-side 2D domain. Spillover across the $m_1 = m_2$ boundary line of Σ (equal-mass boundary line) is a true *penalty*, and thus (d) should be kept to a minimum. This is not the case for the other two boundary lines of Σ, where points beyond $\partial \Sigma$ could well correspond to *possible* (though unlikely) sources.

At *large* values of the minimal match, e.g. typically $M(h,g) \geq \Gamma \gtrsim 0.97$, as prescribed for a single-step search strategy [8], the match is very well approximated by a *quadratic* function [7] of the distance between H and G in parameter space, and the (approximate) match contour lines $\gamma_\Gamma(G)$ are ellipses. However when using post 1PN order waveforms (which will be required in a one-step search to achieve the prescribed *large* minimal-match levels [6]), as G moves throughout Σ, the above ellipses rotate and stretch as an effect of the *intrinsic* nonzero curvature of Σ.

An effective procedure for constructing a 2D spin-free post-1PN template set appropriate to this case has been formulated in [8], as a generalization of the 1PN strategy introduced in [7]. The simplest rectangular-cell template lattice is chosen, and the span of template G_i [i.e. the set of points representing waveforms for which $M(h,g_i) > M(h,g_j), \forall j \neq i$] is accordingly taken as the largest rectangle inscribed in the minimal-match contour line $\gamma_\Gamma(G_i)$. In order to minimize spillover across the equal-mass boundary line of Σ, while optimizing template placement for equal-mass sources (which are credited to be most abundant [10]), the algorithm is started by placing a sufficient number of templates along the equal-mass boundary line. The nearest-neighboring templates are placed in such a way that the boundaries of their rectangular spans *touch* without intersecting. As a result Σ is covered with a set of patches, each of which is a stack of equal-width rectangles, whose height changes according to the shear or stretch of the elliptical γ_Γ contour lines. The current release of GRASP [11] implements a similar procedure, resulting in a relatively straightforward template placement algorithm.

As already noted in [8] the above algorithm is *not* optimal; i.e., it does not necessarily satisfy requirement (b), in view of its *a priori* restriction to rectangular cells [12].

The template placement issue becomes even more complicated at low minimal-match levels (e.g., typically $\Gamma \gtrsim 0.7$) as prescribed in the first step(s) of hierarchical search strategies. In multi-step hierarchical searches a *single* template lattice Λ designed to achieve a *large* Γ throughout Σ is constructed. In the first step only the correlators corresponding to a suitably *decimated* subset of Λ are computed, covering Σ at a *lower* minimal-match level. In the second step, only a limited number of correlators, corresponding to a few nondecimated subsets of Λ, need to be actually computed, covering suitable neighborhood(s) of the candidate signals discovered in the first step. Multi-step hierarchical search strategies should allow a sizable reduction in the required computing power [13–15]. Mohanty [14] formulated a simple strategy for evaluating the lattice decimation steps (taken as constant throughout extended patches of the lattice) for a post-1PN template lattice. Also in this case, however, requirement (b) will be most certainly violated. By itself, the

template placement issue at low minimal-match levels is further complicated by the fact that the match contour lines $\gamma_\Gamma(G)$ besides varying with G are *no longer* elliptical. For this reason, the procedure expounded in [14] can only be validated by extensive Monte Carlo trials.

In this paper we present a possible way to get rid of all the above difficulties and limitations, by capitalizing on the remarkable properties of the post-1PN waveform parametrization introduced by Tanaka and Tagoshi [16], and further discussed in [17]. We accordingly introduce a simple and systematic procedure to set up an optimum template-lattice [18], which closely satisfies *all* conditions (a), (b) and (c) above, at *any* prescribed minimal-match level [19].

The paper is organized as follows. In Sec. II the Tanaka-Tagoshi parametrization and its relevant properties, including the main features of the match contour lines, are briefly introduced. In Sec. III our optimum template placement procedure is exposed in detail. In Sec. IV the gain achievable by cardinal interpolation among these optimally placed templates is discussed. Conclusions follow in Sec. V.

II. TANAKA-TAGOSHI PARAMETRIZATION OF POST-1PN WAVEFORMS

The Tanaka-Tagoshi transformation [20] is a linear one-to-one mapping $F \in \Sigma \leftrightarrow \tilde{F} \in \mathcal{T}$ between the (2D, spin-free, post-1PN) admissible waveform parameter space Σ and a *globally flat* manifold $\mathcal{T}$ such that (i) the ratio

$$\epsilon = \left| \frac{M(h,g) - M(\tilde{h},\tilde{g})}{M(h,g)} \right| \qquad (2.1)$$

is *negligibly small* (typically of the order of 10^{-3} [17]) and (ii) $M(\tilde{h},\tilde{g})$ depends *only* on the *distance* between $\tilde{H}$ and $\tilde{G}$ [16]. The Tanaka-Tagoshi construction is effective for all first generation interferometers [17].

Clearly, property (i) above allows us to solve the optimum template placement problem in the *globally flat* manifold $\mathcal{T}$, by finding a set $\tilde{\Lambda} = \{\tilde{G}_i\} \subset \mathcal{T}$ such that

$$\cup_i S_\Gamma(\tilde{G}_i) \supseteq \mathcal{T}. \qquad (2.2)$$

On the other hand, property (ii) implies that the sets $S_\Gamma(\tilde{G}_i)$ are *identical* up to trivial translations. This means that $\tilde{\Lambda} \subset \mathcal{T}$ is a *globally uniform* template lattice, featuring a *regular* grid of nodes, at *any* prescribed minimal-match level.

A. Constant match contour lines in Tanaka-Tagoshi coordinates

The match contour lines $\gamma_\Gamma(\tilde{G})$ in the (dimensionless) Tanaka-Tagoshi (spin-free) waveform parameter-space coordinates (x_1, x_2) have different geometrical features, depending on the value of Γ. In Fig. 1 the inverse of the curvature radius ρ_γ of $\gamma_\Gamma(\tilde{G})$ is displayed as a function of the polar angle ϕ around $\tilde{G}$ for several representative values of Γ, for LIGO-I at 2.5PN order. The contour lines γ_Γ are also shown in the insets, where $\delta x_i = x_i^{(\tilde{G})} - x_i^{(\tilde{H})}$.
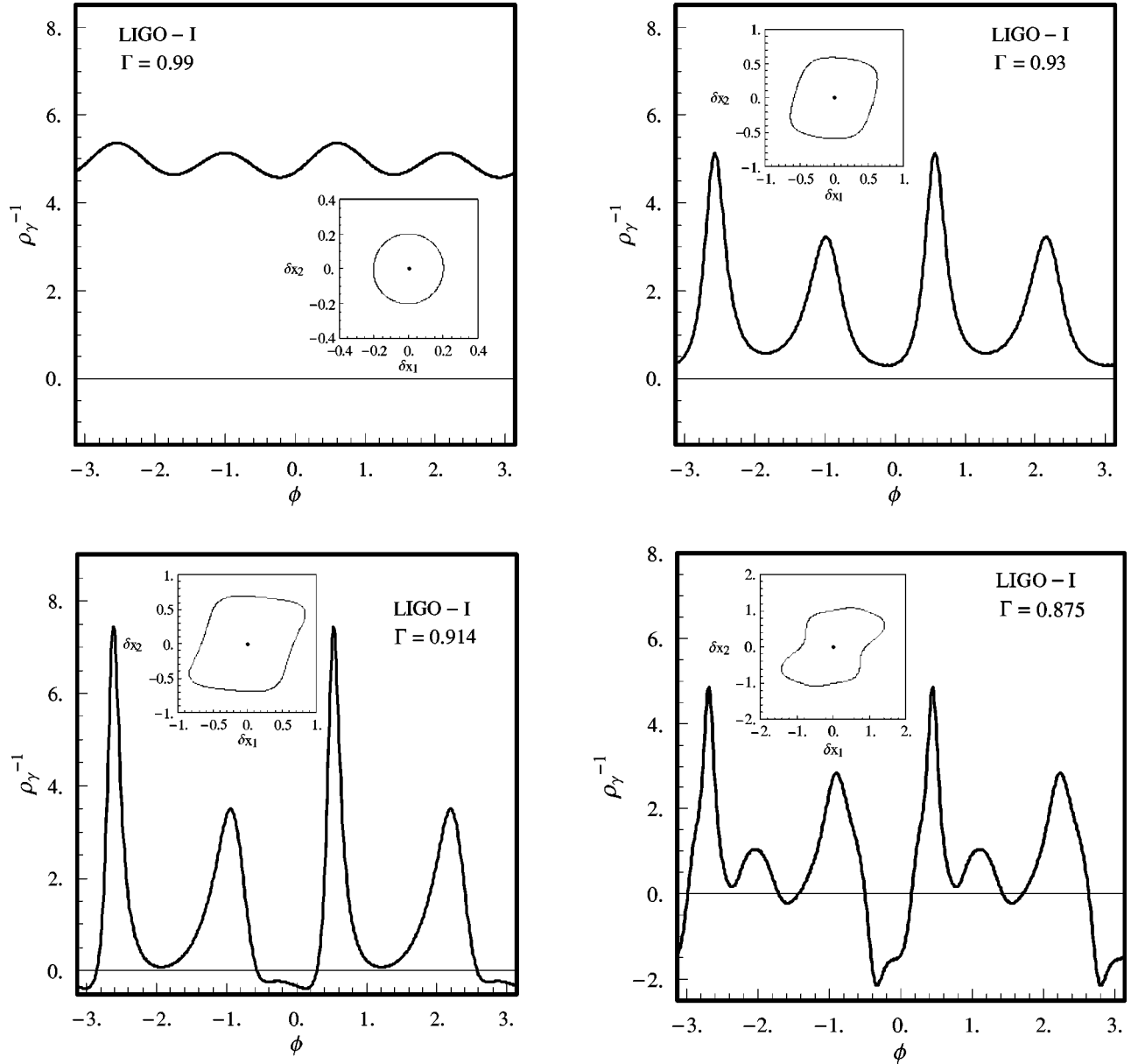
FIG. 1. Match contour lines in Tanaka-Tagoshi coordinates. Curvature ρ_γ^{-1} of γ_Γ vs polar angle ϕ (LIGO-I, 2.5PN).

In the limit as $\Gamma \to 1$ the contour lines γ_Γ are asymptotically circular and ρ_γ^{-1} is almost constant. See, e.g., the $\Gamma = 0.99$ contour line in Fig. 1, top left.

In a range $\Gamma^* \leqslant \Gamma < 1$, the contour lines γ_Γ deviate from circular, but still remain *globally convex*. For LIGO-I, $\Gamma^* \approx 0.9225$. Correspondingly, ρ_γ^{-1} remains *non-negative* throughout a full rotation around $\widetilde{G}$. See, e.g., the $\Gamma = 0.93$ contour line in Fig. 1, top right.

For $\Gamma < \Gamma^*$, the γ_Γ contour lines are *no longer globally convex*. In a range $\Gamma^\dagger < \Gamma < \Gamma^*$, they consist simply of two convex [21] arcs and two concave ones joining smoothly, to form a "peanut" shape. See, e.g., the $\Gamma = 0.914$ contour line in Fig. 1, bottom left. For LIGO-I, $\Gamma^\dagger \approx 0.9109$. As Γ is decreased below $\Gamma^\dagger$, the contour lines become more and more complicated, as more and more bumps and dents appear. Correspondingly, the boundary curvature ρ_γ^{-1} exhibits more and more turning points throughout a full rotation around $\widetilde{G}$. See, e.g., the $\Gamma = 0.875$ contour line in Fig. 1, bottom right.

For all values of Γ, the surface $S_\Gamma(\widetilde{G})$ has always a center of symmetry in $\widetilde{G}$.

III. OPTIMUM TEMPLATE PLACEMENT

In the following we shall discuss the optimum template placement strategy for each of the above-mentioned minimal-match ranges. Optimum here and henceforth means that requirements (a), (b) and (c) discussed in Sec. I will be strictly satisfied [19].

A. Asymptotic $\Gamma \to 1$ limit

In the asymptotic limit $\Gamma \to 1$, the match contour lines are circular. Rotational symmetry of the match contour lines im-
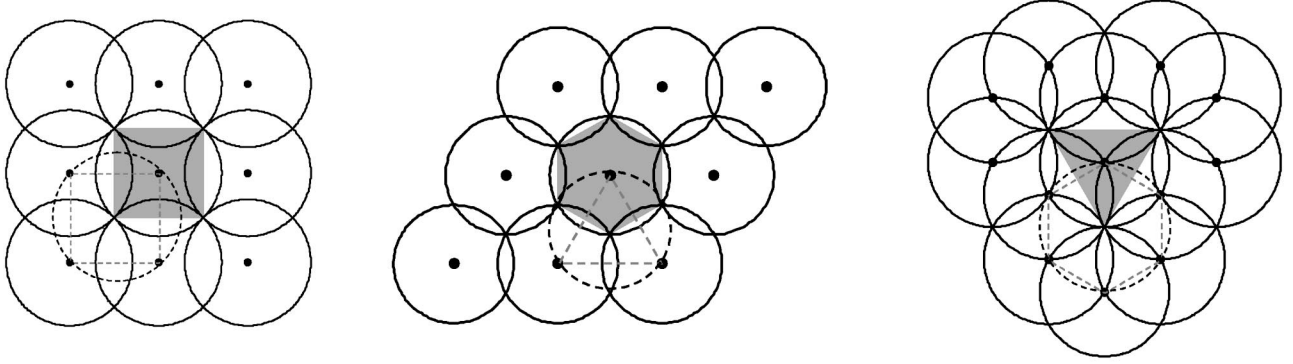
FIG. 2. Triangular, square and hexagonal tilings and pertinent Voronoi sets.

plies that the templates should sit at the vertices of *regular* polygons in the waveform parameter space. These regular (open) polygons should besides make up a (regular) *tiling* of the (Tanaka-Tagoshi) plane [22], and hence can only be triangles, squares or hexagons. Let U be one such polygon and $\{\tilde{G}_i\}$ its vertices. The sparsest templates satisfying Eq. (2.2) are such that the circles $\gamma_\Gamma(\tilde{G}_i)$ touch at a *single* point P, which is obviously the center of symmetry of U. This means that the curve $\gamma_\Gamma(P)$ goes through all the $\tilde{G}_i$'s. Hence, the templates should be located at the vertices of a regular triangle, square or hexagon inscribed in a circle γ_Γ.

The obvious question is which polygon is *best* in terms of the total number of templates needed to cover the admissible-waveform parameter space $\mathcal{T}$ in the Tanaka-Tagoshi plane. Clearly, the best polygon will be the one for which the *span* of each (and any) template has the largest measure (area) [23].

The span (or, in more technical language, the Voronoi set [24]) of $\tilde{G}_i$ is the set of points $\tilde{H}$ for which $M(\tilde{h},\tilde{g}_i) > M(\tilde{h},\tilde{g}_j)$, $\forall j \neq i$, which are the images in the Tanaka-Tagoshi plane of those waveforms h which will be detected using template g_i. The Voronoi sets are shown shaded in Fig. 2, for the (regular) triangular, square and hexagonal tilings of the (Tanaka-Tagoshi) plane [25].

A choice can be made on the basis of a comparison among the measures (areas) of the pertinent Voronoi sets. Let $\mu(\cdot)$ denote the measure (area), $U^{(p)}$ the p-gonal tiling cell, and $V^{(p)}$ the corresponding Voronoi set. It is readily seen that [26]

$$\frac{\mu[V^{(3)}]}{\mu[V^{(4)}]} = 1.299037, \qquad \frac{\mu[V^{(6)}]}{\mu[V^{(4)}]} = 0.649519. \quad (3.1)$$

The triangular tiling is thus seen to be the best choice, yielding a gain in terms of template-span of $\sim 30\%$, whereas the hexagonal one features a loss of $\sim 35\%$, with respect to the simples square tiling [27].

The triangular *tiling* yields a template *lattice* whose fundamental domain (lattice cell) is a parallelogram [18]. Only three vertices of any lattice cell belong to a single curve γ_Γ.

B. Range $\Gamma > \Gamma^*$

In the range $\Gamma > \Gamma^*$, the contour lines $\gamma_\Gamma(\tilde{G})$ are no longer circles, but still *globally convex* and center symmetric. Circular symmetry being lost, we shall still seek the sparsest template collocation subject to Eq. (2.2) among the non-regular, but still center-symmetric (open) p-gons ($p = 3,4,6,$) with all vertices on γ_Γ, which tile the Tanaka-Tagoshi plane.

It makes sense to compare for this case the template-span (Voronoi set) measures (areas) $\mu[V^{(p)}]$, $p = 3,4,6$, to the template-span measure (area) $\mu[V_0^{(4)}]$ of the square tiling [26] pertinent to the naive (but usual) approximation of circular match contour lines. The ratios

$$r_p = \frac{\mu[V^{(p)}]}{\mu[V_0^{(4)}]}, \qquad p = 3,4,6, \qquad (3.2)$$

are displayed in Fig. 3 as functions of Γ for LIGO-I. Not unexpectedly, the triangular tiling is once more the best. This conclusion is valid for all first generation antennas, and the pertinent values of r_3 have been collected in Table I.
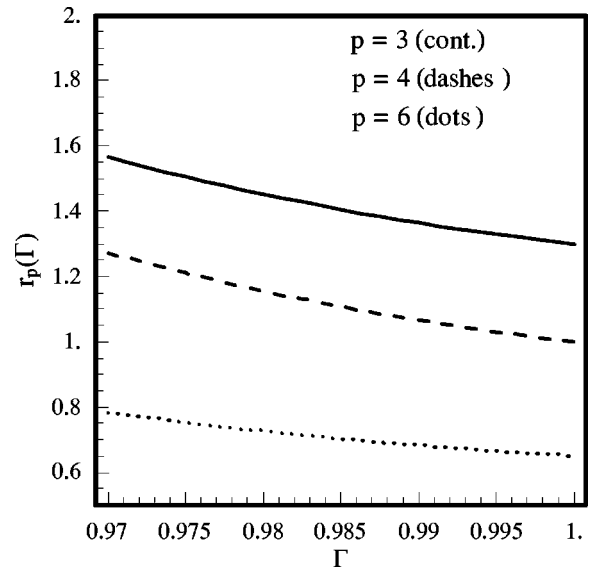

FIG. 3. The ratios r_p, $p = 3,4,6$ relevant to Eq. (3.2) as functions of Γ (LIGO-I, 2.5PN).

Antenna	r_3
TAMA300	1.58
LIGO-I	1.43
GEO600	1.58
VIRGO	1.38

C. Range $\Gamma < \Gamma^*$

By an argument of continuity (i.e. since the match contour lines corresponding to $\Gamma < \Gamma^*$ can be obtained from those corresponding to $\Gamma > \Gamma^*$ by continuous transformations) we shall still seek the optimum tiling of Tanaka-Tagoshi plane using the (open) triangles with (all) vertices on γ_Γ. However, the match contour lines being no longer globally convex, the *largest-area* triangle inscribed in γ_Γ does *not* necessarily cope with Eq. (2.2), as e.g. exemplified in Fig. 4.

One should accordingly seek three points $\tilde{G}_i$ on γ_Γ yielding the largest-area triangle $\tilde{G}_0 \tilde{G}_1 \tilde{G}_2$, subject to Eq. (2.2). The minimal-match condition (2.2) is equivalent to

$$C - \cup_i [C \cap S_\Gamma(\tilde{G}_i)] = \varnothing, \qquad (3.3)$$

where C is the (parallelogram) fundamental domain of the lattice corresponding to a given triangular tiling. Condition (3.3) is most easily checked, involving only four patches S_Γ.

Let $\tilde{P}, \tilde{P}', \tilde{Q}, \tilde{Q}'$ the points (ordered, e.g., counterclockwise) where γ_Γ and its convex-hull [28] detach, shown in Fig. 5. One can readily prove that two vertices of the sought optimum triangular tile, say $\tilde{G}_0$, $\tilde{G}_1$, should be sought on the arc $\tilde{P}\tilde{P}'$ (or $\tilde{Q}\tilde{Q}'$) of γ_Γ, while the third should be sought on the arc $\tilde{Q}\tilde{Q}'$ (respectively $\tilde{P}\tilde{P}'$). It is also readily proved that the lattice vector $\tilde{G}_0 \tilde{G}_1$, after a trivial translation making its midpoint coincident with $\tilde{G}$, should be contained in the butterfly-shaped region $(\tilde{P}\tilde{G}\tilde{Q}' \cup \tilde{Q}\tilde{G}\tilde{P}') \cap S_\Gamma(\tilde{G})$ depicted in Fig. 5.
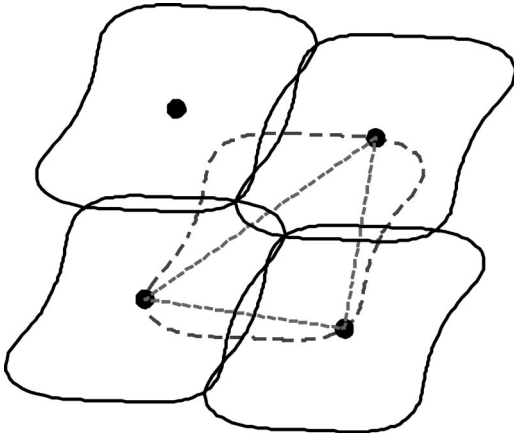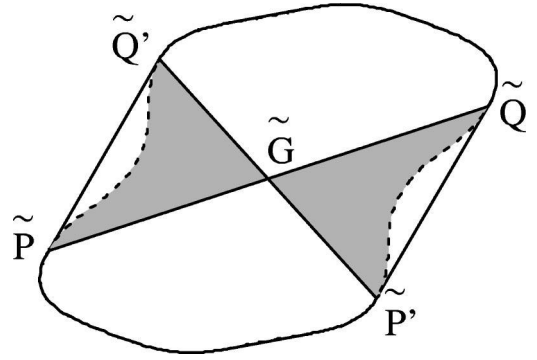

FIG. 5. The butterfly-shaped set $(\tilde{P}\tilde{G}\tilde{Q}' \cup \tilde{Q}\tilde{G}\tilde{P}') \cap S_\Gamma(\tilde{G})$ (LIGO-I, 2.5PN, $\Gamma = 0.875$).

The maximum-area triangular tiles subject to the constraint (2.2), are shown in Fig. 6, for several values of Γ in the range $0.7 \leq \Gamma < 1$ (note that different scales are used in the figure, for better readability). The lattice cell measure corresponding to the optimum triangular tile is displayed in Fig. 7 as a function of Γ, together with the number of templates needed to cover the companion-mass range $0.2 M_\odot \leq m_1 \leq m_2 \leq 10 M_\odot$, for a number of representative minimal-match values.

IV. CORRELATOR BANK ECONOMIZATION VIA CARDINAL INTERPOLATION

In recent papers it has been shown that a sensible reduction ($\approx 75\%$ for 1PN and higher-PN-order templates) in the number of correlators to be computed in order to achieve a prescribed minimal-match can be obtained using cardinal interpolation, thanks to the quasiband-limited property of the match function [29,30]. These results were obtained under the simplest assumption of a square-cell template lattice.

Two obvious questions are now in order: (i) whether and to what extent cardinal interpolation is still effective when using the optimum triangular tiling discussed in the previous
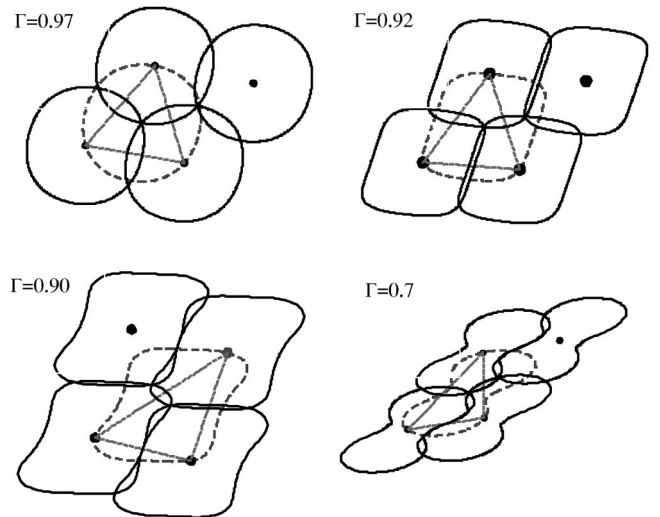

FIG. 4. Inscribed triangle with largest area does not necessarily cope with minimal-match condition for $\Gamma < \Gamma^*$ (LIGO-I, 2.5PN, $\Gamma = 0.9$).

FIG. 6. Optimum triangular tilings and template lattices for several values of Γ (LIGO-I, 2.5PN).

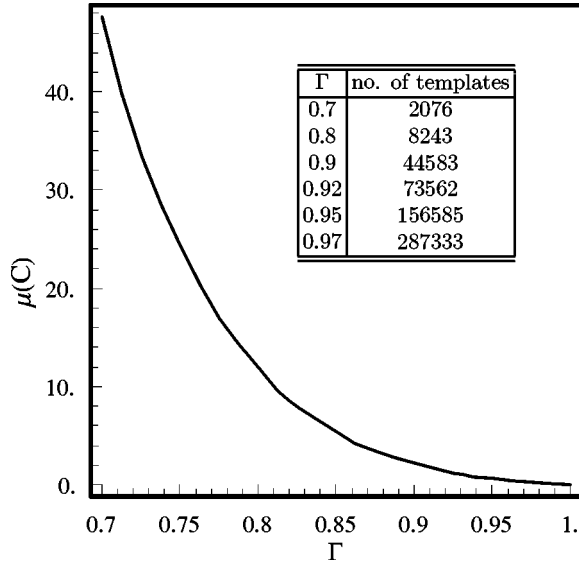| Γ	no. of templates
0.7	2076
0.8	8243
0.9	44583
0.92	73562
0.95	156585
0.97	287333

FIG. 7. Lattice-cell area corresponding to optimum triangular tiling and number of templates needed to cover the range $0.2M_\odot \leq m_1 \leq m_2 \leq 10M_\odot$ vs minimal match (LIGO-I, 2.5PN).

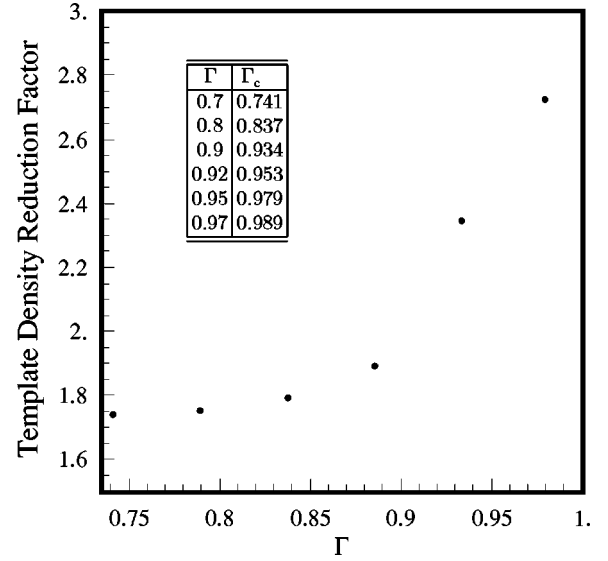| Γ	Γ_c
0.7	0.741
0.8	0.837
0.9	0.934
0.92	0.953
0.95	0.979
0.97	0.989

FIG. 8. Cardinal-interpolation gain (template density reduction factor and minimal-match boost) for optimum triangular tiling (LIGO-I, 2.5PN).

sections [31], and (ii) whether and to what extent cardinal interpolation is still useful at relatively low Γ values, as needed in the early step(s) of hierarchical searches. Numerical simulations have been run to clarify both issues.

In Fig. 8 the template density reduction [32] obtained by cardinal interpolation among optimally placed templates is displayed as a function of the prescribed minimal match Γ. In the inset of Fig. 8, the (boosted) minimal-match values obtained after cardinal interpolation among the optimally placed templates corresponding to a number of representative values of Γ are also listed.

At $\Gamma = 0.97$ a template density reduction ≈ 2.79 is obtained. The apparent discrepancy between this value and the one reported in [30] is readily explained. The template density required to achieve a prescribed minimal match when using cardinal interpolation is essentially independent from the *shape* of the lattice fundamental domain, depending only on its *measure* (area), according to the well-known Nyquist-rate condition [33].

Thus, the template density reduction ≈ 4 in [30,17] when using the simplest square-cell lattice is seen to result from two factors: a factor ≈ 2.79, expressing the template density

reduction due to cardinal interpolation when using the *optimum* triangular tiling, times a factor ≈ 1.43 expressing the template density reduction implied in using the optimum triangular tiling instead of the simplest square one.

V. CONCLUSIONS

We presented a simple and systematic procedure for constructing the sparsest lattice of templates subject to a given minimal-match constraint in the range from $\Gamma \sim 1$ down to $\Gamma \approx 0.7$ (and below) in the (spin-free) Tanaka-Tagoshi parameter space of post-1PN gravitational wave chirps.

We also showed that cardinal interpolation can be effective for correlator-bank economization both in the late and early stage(s) of multi-step hierarchical searches.

ACKNOWLEDGMENTS

[1] B.F. Schutz, Class. Quantum Grav. **16**, A131 (1999).

[2] T. Damour, B.R. Iyer, and B.S. Sathyaprakash, Phys. Rev. D **63**, 044023 (2001).

[3] C. W. Helström, *Statistical Theory of Signal Detection* (Pergamon, Oxford, 1968).

[4] B.S. Sathyaprakash and S.V. Dhurandhar, Phys. Rev. D **44**, 3819 (1991).

[5] S.V. Dhurandhar and B.S. Sathyaprakash, Phys. Rev. D **49**, 1707 (1994).

[6] T.A. Apostolatos, Phys. Rev. D **52**, 605 (1995).

[7] B.J. Owen, Phys. Rev. D **53**, 6749 (1996).

[8] B.J. Owen and B.S. Sathyaprakash, Phys. Rev. D **60**, 022002 (1999).

[9] The maximization is trivially accomplished by taking the largest absolute element in the (inverse, fast) discrete Fourier transform of $h(f)g^*(f)/\Pi(f)$ [7].

[10] J.H. Taylor, Rev. Mod. Phys. **66**, 711 (1994).

[11] GRASP is the current *de facto* standard software package for gravitational wave data analysis, available from http://www.lsc-group.phys.uwm. edu/~ballen/grasp-distribu-

tion.

[12] It should be noted that template *overpopulation* even in a *subset* of the waveform parameter space increases the false-alarm probability of the *whole* bank, at a fixed detection threshold level.

[13] S.D. Mohanty and S.V. Dhurandhar, Phys. Rev. D **54**, 7108 (1996).

[14] S.D. Mohanty, Phys. Rev. D **57**, 630 (1998).

[15] Multi-step searches could be implemented following different routes. One might alternatively use lower PN-order templates in the early stage(s) to obtain a coarse estimate of (a subset of) candidate-event source parameters, and then use the best-available higher-PN-order templates for a refined high-Γ search in the neighborhood(s) of the candidate source(s) sieved in the first step. No quantitative analysis of this procedure has been given yet. See A.E. Chronopoulos and T.A. Apostolatos, Phys. Rev. D **64**, 042003 (2001), for an updated discussion of the problem of matching waveforms of different PN orders.

[16] T. Tanaka and H. Tagoshi, Phys. Rev. D **62**, 082001 (2000).

[17] R.P. Croce, Th. Demma, V. Pierro, and I.M. Pinto, Phys. Rev. D **64**, 042005 (2001).

[18] A 2D (regular) lattice is the set of intersections between two (non-parallel) sets of parallel equispaced lines. The resulting checkerboard tiles the plane with (equal) parallelograms. Any of these parallelograms is the lattice *fundamental cell*. The two vectors from any grid node to its nearest-neighbor fundamental-cell vertices are the *lattice vectors*.

[19] The template spillover condition (d) will be approximately satisfied at the same level of accuracy provided by current placement algorithms.

[20] Basically, the Tanaka-Tagoshi transformation is obtained by requiring $\mathcal{T}$ to touch Σ at its three vertices. See Appendix B of [17] for details.

[21] Convex (concave) arc here means that the (open) segment between the arc end points is completely included in (respectively, external to) S_Γ.

[22] A (polygonal) tiling of R^2 is a countable family of (open) polygons U_i, which (i) are disjoint and (ii) are such that their closures cover R^2. In a *regular* tiling all tiles U_i are congruent,

i.e. can be made to coincide up to suitable translations and rotations.

[23] The total number of templates needed to cover $\mathcal{T}$ is approximately equal to the ratio between the measure (area) of Σ and the measure (area) of the template *span*.

[24] Given a set of points $\mathcal{G} \subseteq R^n$, the Voronoi set or *proximity locus* of $G_k \in \mathcal{G}$ is the set $V(G_k) = \{x \in R^n : \forall h \neq k, D(x, G_h) > D(x, G_k)\}$, where $D(\cdot, \cdot)$ is a suitable distance (metric).

[25] It is seen from Fig. 2 that, but for trivial translations, $U^{(3)} = V^{(6)}$, $U^{(6)} = V^{(3)}$, and $U^{(4)} = V^{(4)}$; i.e., the triangular and hexagonal tiling are Voronoi dual, while the square tiling is Voronoi self-dual.

[26] We remind the reader that for circular match contour lines, the inscribed square-tile area is given by $\mu[V^{(4)}] = 2(1-\Gamma)$.

[27] Occasional confusion is made in the technical literature between the tiling cell and tiling-cell's span (Voronoi set) measures, leading e.g. to the often quoted statement that hexagonal tiling would be the most efficient.

[28] The convex hull of a set U is the smallest convex set containing U.

[29] R.P. Croce, Th. Demma, V. Pierro, I.M. Pinto, and F. Postiglione, Phys. Rev. D **62**, 124020 (2000).

[30] R.P. Croce, Th. Demma, V. Pierro, I.M. Pinto, D. Churches, and B.S. Sathyaprakash, Phys. Rev. D **62**, 121101(R) (2000).

[31] The standard 2D cardinal-interpolation formula applies to the case where the interpolation points form a rectangular grid. The cardinal-interpolation formula for the case where the interpolated points form a skew grid is more or less obviously obtained by first applying a trivial coordinate transformation which brings the grid into a rectangular one, then writing down the usual (rectangular-grid) cardinal-interpolation formula, and finally switching back to the original coordinates.

[32] The template-density reduction factor is defined here as the ratio between the areas of the (optimal) triangular tiles yielding the same minimal match with and without cardinal interpolation.

[33] See, e.g., J. R. Higgins, *Sampling Theory in Fourier and Signal Analysis* (Clarendon Press, Oxford, 1996), chap. 14.